Chapter 27

Seismic Microzonation

大徳寺孤篷庵　忘筌

Koho-An of Daitoku-Ji Temple in Kyoto. This Zen temple invites people into a metaphysical world. The room and the garden in the photograph compose a symbolized sea as viewed from a boat; the paper screen at the top suggests the side board of a boat while the garden outside is the sea.

27.1 Microzonation for Intensity of Earthquake Motion

Seismic zonation or microzonation stands for assessing and classifying the extent of risk in localities by taking into account the expected nature of future earthquakes as well as topography, soil conditions, and other individual conditions. The name may or may not carry "micro", depending upon the size of considered localities. This section concerns in particular the risk that is related to such earthquake problems as intensity of earthquake motion and liquefaction. Topics concerning landslide risk assessment were discussed in Sect. 15.46. Design requirements as well as emergency program after an earthquake disaster should take into account the microzonation so that relevant action may be taken for each localities. A good reference on this topic was published by the Technical Committee No. 4 for Earthquake Geotechnical Engineering under the auspices of International Society for Soil Mechanics and Geotechnical Engineering (ISSMGE) (1999). Most parts of this chapter rely on this report.

The quality and reliability of risk assessment depend on the amount of investigation and data interpretation. It is, therefore, very likely that high reliability is not achieved or even not necessary when there are time and financial limitations. Hence, the practice of (micro)zonation is classified into three grade groups; Grade 1 with least labor and Grade 3 that is most elaborate. The practice should choose the most appropriate grade, depending upon the situation and requirement. Differences among grades are described in what follows.

Microzonation begins with the assessment of regional seismic activity. Zoning is more important in tectonically more active region. The probability of an occurrence of a big earthquake in the studied region is assessed by historical records that are converted to, for example, the Gutenberg-Richter (1944) diagram. If historical record for a sufficiently long period of time is not available, an alternative approach may be trench excavation of a fault (Fig. 16.3) and paleoliquefaction (Sect. 18.4) for which the date is determined.

Zonation of grade 1 is carried out by using information and knowledge that are available in literatures. Hence, neither soil investigation nor numerical analysis is required. A typical important information is found in experiences during past earthquakes. For example, Fig. 5.32 illustrated the damage distribution in Tokyo during the 1923 Kanto earthquake. The area of heavy damage rate in this figure agreed with the area of soft and recent alluvial deposits. It is important that the magnitude of amplification in earthquake motion is somehow related with the surface geology. See the experience in California (Fig. 5.7). Figure 27.1, accordingly, illustrates a proposal by Midorikawa (1987), which was derived on the basis of calculated amplification (Sect. 6.8) of ground motion averaged over a certain frequency range. Note that the geological consideration of this type does not pay attention to the thickness of geomaterials. Moreover, since the amplification data were obtained from observation of frequent but weak ground motion, the amplification during a strong shaking may be different from the expectation because of the nonlinearity of soil (Fig. 9.13 and Chap. 10) that becomes significant during strong shaking.

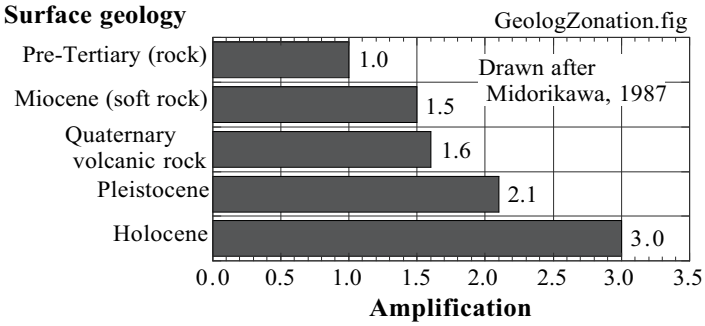

Fig. 27.1 Amplification of earthquake motion in different surface geology (drawn after Midorikawa, 1987)
Note: Amplificaiton in this figure comes from TC4 committee report. Original paper by Midorikawa (1987) gave amplification 2.5 times bigger than those in this figure.

Zonation of grade 2 collects more subsurface data in addition to literature information. For example, SPT-N values are converted to S-wave velocity, $V_s = \sqrt{G_{max}/\rho}$, by using empirical correlations (Sect. 8.4–8.6). By using a V_s profile thus obtained above an engineering base layer, microzonation is carried

out. For example, Shima (1978) indicated that the greater ratio of (V_s in bedrock)/(V_s in surface soil) leads to the greater amplification; softer surface soil generates greater amplification. Noteworthy is that the practical subsurface investigation is seldom conducted down to the real bedrock. It is a common practice to consider a soil layer with $V_s \geq 600$ m/s as an engineering base (rock), although a real rock layer lies far below it. Few engineering soil investigation is conducted below a layer of SPT-$N > 50$ that is a good bearing layer for foundation of structures.

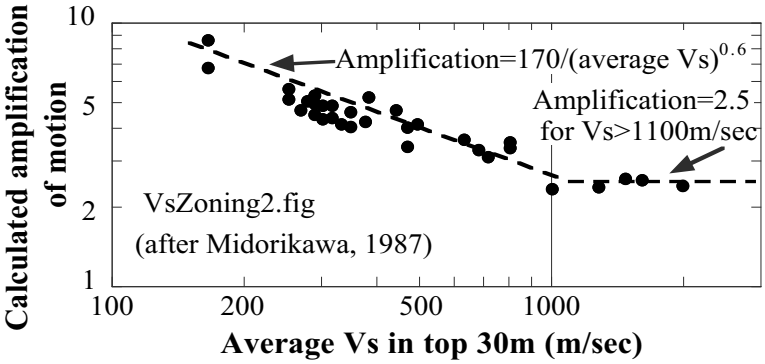

Fig. 27.2 Assessment of amplification of ground motion by average V_s (Midorikawa, 1987)
Note: Amplificaiton in this figure comes from the original paper by Midorikawa. Later, TC4 committee report reduced the amplification to 1/2.5.

T_G is one of the applications of the V_s profile which is defined by

$$T_G \equiv 4 \sum_{\text{surface}}^{\text{base}} \frac{H_i}{V_{si}} \qquad (27.1)$$

where H_i and V_{si} are thickness and V_s of the ith layer in the ground (see (21.4)). Being similar to the natural period of a uniform soil deposit, T_G is expected to help assess the magnitude of amplification (6.30). Table 21.3 in Sect. 21.7 gave an idea of ground classification (microzonation), based on this parameter.

Moreover, it is expected that the mean value of V_s in the surface deposit is approximately related with the amplification of motion averaged over a certain frequency range. Figure 27.2 demonstrates an example formula proposed by Midorikawa (1987).

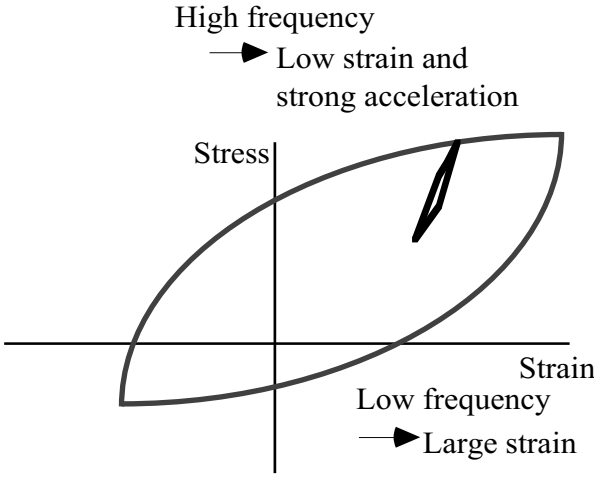

Fig. 27.3 Appropriate rigidity and damping ratio for low- and high-frequency components

A different kind of grade-2 approach is the use of microtremor observation. Figures 8.35 and 8.36 illustrated two examples of microzonation, based on intensity and period of this weak ground vibration.

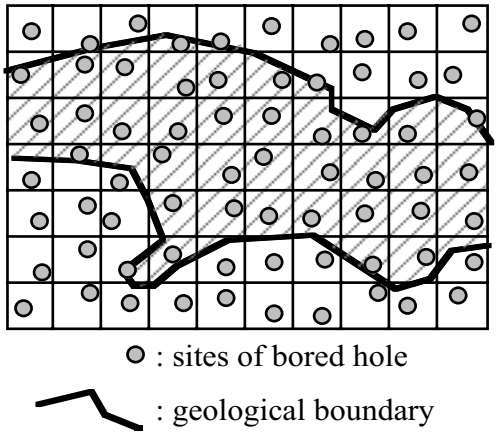

Fig. 27.4 Square grids on more irregular geological conditions

Zonation of grade 3 runs nonlinear dynamic analyses. For simplicity, V_s or $G_{max} = \rho V_s^2$ at small strain amplitude is determined by SPT-N, while nonlinearity is considered by using literature information (Chap. 10). This implies that the equivalent linear analysis (Sect. 9.14) is most frequently employed. However, care is needed in analyses on very soft ground undergoing strong shaking. A commonly encountered problem is that the calculated motion at the surface is stronger upon hard soil than on such soft soil, which appears contradictory to knowledge of damage distribution (Fig. 5.32). The reason for this problem is that the existing computer codes (equivalent linear analysis with complex-modulus modelling) assume equal values of secant shear modulus (G) and damping ratio to all the

frequency components. Since the strain amplitude is large under strong shaking, small G and large damping ratio are assumed. Although these values are reasonable for low-frequency components that generate large strain, they are not appropriate for high-frequency components whose strain amplitude is small but contribution to acceleration is significant (Figs. 9.46 and 27.3). These high-frequency components are unduly decayed by the overestimated damping ratio, and the acceleration at the ground surface is underestimated. Sugito et al. (1994) together with Sugito (1995) proposed to allocate different damping characteristics to different frequency components on the basis of the respective strain amplitudes. Note that some constitutive models that are employed in analyses in the time domain overestimate the energy damping at large strain amplitude as well.

Zoning may be made easy by constructing square grids (Fig. 27.4) in the studied region and determining a representative soil profile in each of them. By using the representative soil profile, one of the above procedures is practiced and the corresponding grid is classified. The problem lying in this procedure is that the geological and topographical boundaries do not necessarily match the boundary of square grids. It is better to determine the zone boundary on the basis of the geological and topographical boundaries.

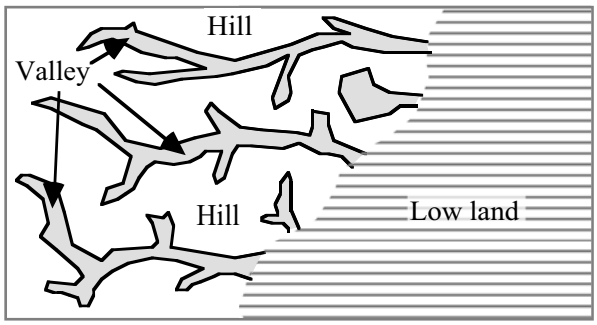

Fig. 27.5 Small valley in pleistocene hilly area

Fig. 27.6 Magome site of Tokyo in small valley

Fig. 27.7 Peaty soil in small valley

Ohsaki (1983) issued a caution on the problem lying in the bottom of a small valley within a hilly area. Figure 27.5 illustrates such a geological condition. Figure 27.6 shows a site in such a small valley. When an excavation was planned in this site, a very soft deposit of peaty soil was encountered (Fig. 27.7). Being too soft for any construction machine to come in, this peat was grouted (Fig. 27.8) and thereinafter a machine came in to excavate. This soft deposit was produced when this place was a small pond in such a valley.

Fig. 27.8 Soil improvement of peaty material by grouting special liquid

27.2 Microzonation for Liquefaction

This section continues the foregoing discussion with an emphasis on liquefaction hazard. There are again three grades in microzonation for liquefaction risk. Grade 1 uses literature and experiences. Therefore, it does not require field investigation.

Figure 18.38 demonstrated the distribution of liquefaction during the earthquake in 1923. It was therein shown that liquefaction-prone geology is the abandoned river channel and the deltaic deposit. Figure 17.34 showed as well the difference in liquefaction resistance between old and recent subsoils in Dagupan, the Philippines. The experience in Kobe in 1995 indicated that recent man-made islands are vulnerable to liquefaction as well (Fig. 18.43). Figure 27.9 illustrates a huge landslide, which was triggered by liquefaction of loess soil (aeolian deposit) during the 1920 earthquake (M=8.5, Wang et al. 2000 and 2001). Therefore, recent loose deposits of cohesionless soil lying under ground water table have high potential to liquefy. In contrast, cohesive soil would not liquefy (Sect. 20.4).

Microzonation of grade 2 relies on more efforts to collect information from unpublished literatures and interview to residents. Youd and Perkins (1978) presented a very elaborate information that is shown in Table 27.1. Liquefaction is unlikely in most dunes because the ground water table is low. It is, however, important that the secondary deposit of dune sand results in high liquefaction susceptibility. The secondary deposit means that dune sand is transported by wind and gravity into low and wet land adjacent to dune hill and develops loose and water-saturated layer.

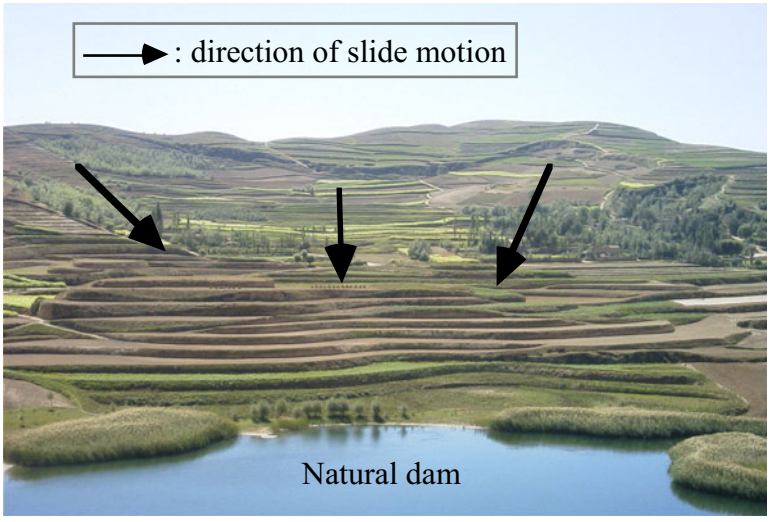

Fig. 27.9 Failure of very gentle loess slope due to earthquake (寧夏回族自治區西吉, Ningxia, China)

Ageing increases the liquefaction resistance (Sect. 18.13). It is, however, true that the rate of this increase varies from region to region, probably depending on the frequency of strong shaking in the particular region (local seismic activity; Sect. 18.13); densification of sand by repeated past earthquakes. Wakamatsu (1992) proposed a similar idea (Table 27.2) on liquefaction susceptibility for the JMA (Japanese Meteorological Agency) seismic intensity scale of *V*.

The grade-3 microzonation for liquefaction hazard is conducted by running subsoil investigation, such as SPT, and necessary calculation or analysis. The factor of safety against liquefaction, F_L, is obtained from SPT-*N* and other bore hole data (Sect. 19.4), which is then converted to a single value (for example, P_L in Sect. 21.9) that represents the bore hole site (Sect. 21.9). Then, microzonation becomes possible. However, the ignorance of local topographical boundaries in a grid operation (Fig. 27.4) should be borne in mind. Attention should be paid to the reliability or details of SPT procedure, which may affect the quality of obtained *N* values.

It is further possible to take into account the risk of lateral displacement of liquefied sand in sloping ground as well as behind an unstable quay wall (Chap. 24). Youd and Perkins (1987) proposed an index of LSI (liquefaction severity index), which is a function of earthquake magnitude, distance from the seismic source, and local geological as well as topographical conditions. Standing for the maximum possible displacement in lateral directions, LSI can be an index to perform microzonation. Note that LSI cannot take into account human efforts to improve soil conditions and to mitigate liquefaction problems.

Table 27.1 Liquefaction susceptibility in different surface geology (original table by Youd and Perkins, 1978, was modified and/or summarized by the author) (author´s remarks are shown in the foot note)

Type of deposit	Susceptibility to liquefaction when saturated with water.			
	Age < 500 years	Holocene	Pleistocene	Older than Pleistocene
Inland deposits				
River channel	Very high	High	Low	Very low
Flood plain	High	Moderate	Low	Very low
Alluvial fan and plain [a]	N/A	Low	Very low	Very low
Marine terraces and plains	Moderate	Low	Low	Very low
Delta and fan delta	High	Moderate	Low	Very low
Lacustrine and playa	High	Moderate	Low	Very low
Colluvium	High	Moderate	Low	Very low
Talus	Low	Low	Very low	Very low
Dune [b]	High	Moderate	Low	Very low
Loess [c]	High	High	High	Very low
Glacial till	Low	Low	Very low	Very low
Tuff [d]	Low	Low	Very low	Very low
Tephra	High	High	?	?
Residual soil	Low	Low	Very low	Very low
Coastal deposits				
Delta	Very high	High	Low	Very low
Estuarine	High	Moderate	Low	Very low
Beach [e]				
high wave energy	Moderate	Low	Very low	Very low
low wave energy	High	Moderate	Low	Very low
Lagoon	High	Moderate	Low	Very low
Fore shore	High	Moderate	Low	Very low
Artificial deposits or land reclamation				
Not densified	Very high	N/A	N/A	N/A
Densified / compacted	Low	N/A	N/A	N/A

a: Be careful of small former river channel, etc.
b: Most dune sand lies above ground water and is unlikely to liquefy. However, be careful of low and wet low lands between dune hills.
c: Loess slope failed easily (Fig. 27.9).
d: Normally volcanic ash is hot upon deposition near the crater and develops bonding.
e: Beach sand is compacted by wave energy

Table 27.2 Susceptibility of soil to liquefaction in a variety of geomorphological units undergoing JMA seismic intensity scale of V (Wakamatsu, 1992)

Geomorphological conditions		Possibility to
Classification	Specific condition	liquefy
Valley plain	Valley plain consisting of gravel or cobble	Not likely
	Valley plain consisting of sandy soil	Possible
Alluvial fan	Vertical gradient of more than 0.5%	Not likely
	Vertical gradient of less than 0.5%	Possible
Natural levee	Top of natural levee	Possible
	Edge of natural levee[a]	Likely
Back marsh		Possible
Abandoned river channel		Likely
Former pond		Likely
Marsh and swamp		Possible
Dry river bed	Dry river bed consisting of gravel	Not likely
	Dry river bed consisting of sandy soil	Likely
Delta		Possible
Bar	Sand bar	Possible
	Gravel bar	Not likely
Sand dune	Top of dune	Not likely
	Lower slope of dune	Likely
Beach	Beach	Not likely
	Artificial beach	Likely
Interlevee lowland		Likely
Land reclaimed by drainage		Possible
Reclaimed land		Likely
Spring		Likely
Fill	On boundary between sand and lowland	Likely
	Adjoining cliff	Likely
	On march or swamp	Likely
	On drained and reclaimed land	Likely
	Other type of fill	Possible

a: Figure 17.34 illustrated a boundary between natural levee and more recent deposit. Significant ground failure, probably due to liquefaction, occurred only in the latter geology. Figures 17.56 and 18.40 showed liquefaction in the area of young land reclamation in Dagupan, while Fig. 18.41 demonstrated that natural levee had more resistance against liquefaction.

List of References in Chapter 27

Gutenberg, B. and Richter, C.F. (1944) Frequency of earthquakes in California, Bull. Seism. Soc. Am., Vol. 34, pp. 185-188.

Midorikawa, S. (1987) Prediction of isoseismal map in the Kanto Plain due to hypothetical earthquake, J. Struct. Eng., JSCE, Vol. 33B, pp. 43-48 (in Japanese).

Ohsaki, Y. (1983) Earthquake and Building, Iwanami Shinsho Books, No. 240, p. 179 (in Japanese).

Shima, E. (1978) Seismic microzoning map of Tokyo, Proc. 2nd Int. Conf. Microzonation, Vol. 1, pp. 433-443.

Sugito, M. (1995) Frequency dependent equivalent strain for equi-linearized technique, Proc. First Int. Conf. Earthq. Geotech. Eng., Tokyo, Vol. 2, pp. 655-660.

Sugito, M., Goda, H. and Masuda, T. (1994) Frequency dependent equi-linearized technique for seismic response analysis of multi-layered ground, Proc. JSCE, 493/III-27, pp. 49-58 (in Japanese).

Technical Committee for Earthquake Geotechnical Engineering (TC4 of Int. Soc. Soil Mech. Geotech. Eng.) (1999) Manual for zonation on seismic geotechnical hazard, Revised version.

Wakamatsu, K. (1992) Evaluation of liquefaction susceptibility based on detailed geomorphological classification, Proc. Ann Meet. Arch. Inst. Japan, Vol. B, pp. 1443-1444 (in Japanese).

Wang, L.-M., Hwang, H., Lin, Y., Ryashenko, T.G. and Akulova, V.V. (2001) Comparison of liquefaction potential of loess in China, USA, and Russia, CD-ROM Proc. 4th Int. Conf. on Recent Advances in Geotech. Earthq. Eng. Soil Dynam., San Diego, Paper No. 4.04.

Wang, L.-M., Yuan, Z.-X. and Wang, J.L.L. (2000) The effect to densify on seismic subsidence of loess, CD-ROM Proc. 12th WCEE, Auckland, Paper No. 1319.

Youd, T.L. and Perkins, D.M. (1978) Mapping liquefaction-induced ground failure potential, J. Geotech. Eng., ASCE, Vol. 104, GT4, pp. 433-446.

Youd, T.L. and Perkins, D.M. (1987) Mapping of liquefaction severity index, J. Geotech. Eng, ASCE, Vol. 113, No. 11, pp. 1374-1391.